

# STAMP-ASSISTED GRAVURE PRINTING OF MICRO-SUPERCAPACITORS WITH GENERAL FLEXIBLE SUBSTRATES

Haobin Wang<sup>1,†</sup>, Yu Song<sup>1,†</sup>, Liming Miao<sup>1</sup>, Ji Wan<sup>1</sup>, Xuexian Chen<sup>1,2</sup>, Xiaoliang Cheng<sup>1</sup>, Hang Guo<sup>1,2</sup> and Haixia Zhang<sup>1,2,\*</sup>

<sup>1</sup>National Key Laboratory of Science and Technology on Micro/Nano Fabrication, Institute of Microelectronics, Peking University, Beijing, CHINA

<sup>2</sup>Academy for Advanced Interdisciplinary Studies, Peking University, Beijing, CHINA

## ABSTRACT

In this paper, we present a scalable and general fabrication for micro-supercapacitors (MSCs) among various flexible substrates assisted by the stamp, which combines the conductive polymer composites with gravure printing process. Compared with the traditional transferring techniques, this method greatly simplifies the process and mitigates the mechanical damage during the preparation. Profiting from the composites of carbon nanotubes (CNTs) and polydimethylsiloxane (PDMS) as the printing inks, the MSCs exhibit elegant areal capacitance ( $10.491 \mu\text{F}/\text{cm}^2$ ) on the paper substrate. Meanwhile, optimizing the ratio of matrix and curing agent of PDMS, the interaction between ink and substrate is effectively enhanced. Therefore, such novel fabrication technology significantly improves the production efficiency as well as broadens the applications.

## INTRODUCTION

The pursuit of the wearable ability of personal electronics [1-3] stimulates the intensive researches endeavor to seek highly compact energy storage devices with state-of-the-art performance [4,5]. For the conventional lithium-ion batteries, though the high energy densities are quite desirable [6], the rate of charge/discharge process is restricted. MSCs, the promising candidate in much higher power densities [7-9], generally exhibit a longer lifetimes (over 100,000 cycles) [10,11], thus proving the great potential to be employed as the major power sources of the miniaturized devices.

Compared to the traditional sandwiched structure, the in-planar MSCs with interdigital design are able to shorten the ion transport channel between the electrolyte and the electrodes, as well as maximize the use of active material surfaces [12], which account for the high-profile performance. On this basis, to meet the demands for wearable electronics, such MSCs are required to develop towards simpler process.

Conventionally, the process of preparing MSCs by mask replication is relatively laborious and introducing unnecessary marginal damage. Printing technology as a solution-based processing method, which could realize high throughput of functional patterns with precise structures, is gradually used to fabricate high-performance MSCs [13,14].

Herein, we choose the gravure printing [15,16], a typical method, to improve the integrity and resolution of transferring electrodes of MSCs. With the assistance of the stamp mold, the electrodes of MSCs could be elaborately patterned among various substrates in a low-cost and high-effective way. Besides, cooperating with CNT-PDMS composites [17,18] in appropriate proportion, our work satisfies the requirements of modernization of MSCs.

## EXPERIMENTAL METHODS

Schematic diagram of the MSCs fabrication is shown in Fig. 1, which demonstrates the mass-production of MSCs concisely and the overall structure of as-formed device. It is worth mentioning that the whole transferring process is solution-based and easily controlled on the flexible substrate. Large quantities of devices would be produced in a short time without the complicated extra equipment and procedures.

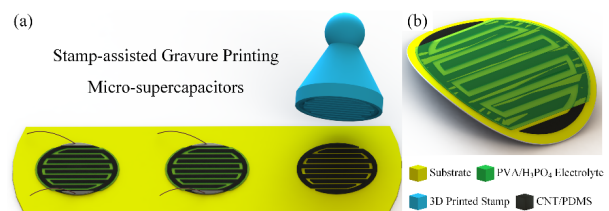


**Figure 1:** (a) Schematic diagram of the MSCs fabricated by gravure printing, and (b) flexible view of the structure.

## Material preparation

The preparation of the CNT-PDMS ink is essential for the entire gravure printing process. For the specific formulation, 3 g elastomer of commercial PDMS (Sylgard 184, Dow Corning Co.) and 300 mg of CNTs (Boyu Co.) are firstly dissolved in the toluene at a polymer/solvent concentration of 20%. The mixture is magnetic stirred approximately for 4 h at the room temperature until the CNTs are mixed into PDMS thoroughly with the help of toluene.

Then the mixture is poured into a culture dish to evaporate partial toluene. Meanwhile, 300 mg cross-linker of PDMS is added with further magnetic stirring around 0.5 h, until the viscosity of CNT-PDMS ink is similar to the commercial ink, which is mainly dominated by the content of the residual toluene.

As for the solid-state electrolyte, it is prepared by adding polyvinyl alcohol (PVA) powder (6 g) into  $\text{H}_3\text{PO}_4$  aqueous solution (6 g  $\text{H}_3\text{PO}_4$  into 60 ml deionized water). The whole mixture is heated to  $85^\circ\text{C}$  under vigorous stirring until the solution becomes clear.

## Fabrication of MSC device

The whole detail gravure printing of the MSC device is demonstrated in Fig. 2. Fabrication process begins by 3D-printing resin stamp as mold (Fig. 2(a)), which is designed using Solidworks 2016, and then issued to the foundry (WeNext Technology Co., Ltd) for processing. Followed by spraying with a thin layer of release agent (Shanghai Smarttech Co., Ltd) on the surface of stamp base to enhance the integrity of gravure transferring.

Then, the stamp dips into the CNT-PDMS ink adequately (Fig. 2(b)). Utilize a doctor blade to remove the excess ink on the surface of stamp (Fig. 2(c)). It is noted that fully removing the ink is challenging due to the persistence of thin lubrication layer of ink [19], meanwhile, the thickness of the lubrication layer can be minimized with proper selection of the doctor blade configuration, ink properties and speed. Next, stamp brimmed with ink is completely printed on the flexible substrate (Fig. 2(d)). After removing the stamp, only the ink in the recessed groove is transferred to the substrate (Fig. 2(e)). Finally, gel electrolyte consisting of PVA and H<sub>3</sub>PO<sub>4</sub> is spray-coated among the interdigital electrodes (Fig. 2(f)) to form the MSCs.

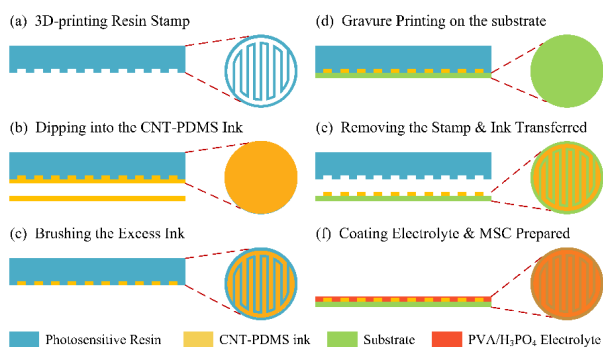


**Figure 2: Fabrication process of interdigital electrodes and flexible MSCs assisted with the 3D-printing stamp.**

### Measurement and Analysis

The morphologies, structure of each layer and the interdigital MSCs are all observed using a scanning electron microscope (SEM) (Quanta 600F, FEI Co.). All of the electrochemical tests of the MSCs are carried out by a three-electrode system using CHI660C (CH instrument) electrochemical workstation at room temperature. As for the mechanical tests or cycle stability tests, an auxiliary tensile stage is used to make MSCs generate mechanical deformations.

## RESULTS AND DISCUSSION

### Optical and SEM analysis

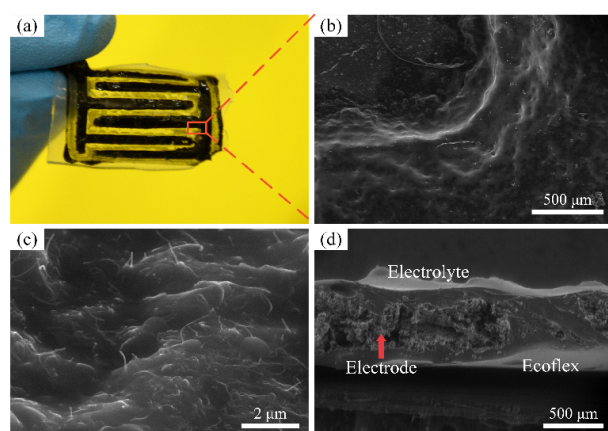


**Figure 3: (a) Digital image of the flexible device. SEM image of the (b) neat-edge of electrodes and (c) CNTs exposed on the surface. (d) The cross section of SEM image of the device.**

With the proposed protocol, the flexible MSC with patterned electrodes has been fabricated (Fig. 3(a)). Remarkably, the MSC processes a well-defined shape, which could be easily deformed and meet the demands in portable electronics.

In addition, the SEM images in Fig. 3(b)-3(c) clearly demonstrate the neat-edge of electrodes and inextricably intertwined CNTs exposed on the surface, which proves the existence of the electric double-layer due to the capacity of ion/charge exchange. The cross-section SEM image of the device shows the detailed structure composed of electrode layer and solid-state electrolyte film, where the electrolyte is penetrated into the electrode to enhance the ion exchange (Fig. 3(d)).

Furthermore, to explore the versatility of the process, more patterns of MSC's electrodes and substrates have been tried. Fig. 4 clearly depicts the MSCs in two sleek shapes on the various substrates. The content of CNT plays a vital role in the entire process, as which increases, the contact between the electrodes and substrate deteriorates, even like the circular-shaped MSC (C-MSC) on the PDMS substrate, a patch of electrode is exfoliated. Whereas, in order to ensure the electrochemical performance, the content of 10 wt% is satisfied.

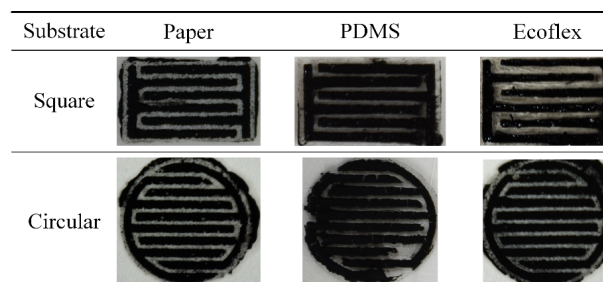


**Figure 4: Optical images of different shapes of interdigital MSCs produced on the various substrates.**

### Electrochemical analysis

With regard to the electrochemical performance of the flexible MSCs in simple process, the devices are detailed evaluated through cyclic voltammetry (CV), galvanostatic charging/discharging tests (GCD), Ragone plots, cycling stability as well as mechanical stability tests via the electrochemical workstation. At first, the C-MSCs on the paper substrate are analyzed by CV curves with the scan rates from 10 mV/s to 200mV/s at a stable potential window between 0 and 1 V (Fig. 5(a)). Quasi-rectangular shapes could be observed due to the characteristic of the CNT-based materials.

Then GCD test is implemented to visually reflect the rates of charging/discharging process in Fig. 5(b). Evidently, the charging curves are symmetrical with their corresponding discharging counterparts, in the case of the currents range from 0.3 μA to 2 μA. Besides, the excellent quasi-linear voltage-time profiles profit from the electric double-layer effect of formed MSCs.

Fig. 5(c) expresses the cycling stability of the C-MSC with interdigital electrodes during the periodic charging/discharging cycles (100 mV/s). Distinctly, more than 90% of the initial capacitance is maintained after 2,000 cycles of CV test.

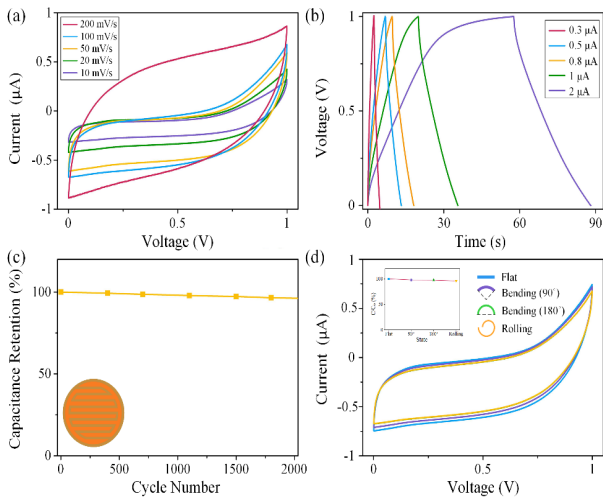


**Figure 5: Electrochemical performance of the MSC in circular shape on the paper substrate.**

To confirm the feasibility as the energy storage component in the field of flexible electronics, the C-MSCs are tested under different mechanical deformation. From Fig. 5(d), there are negligible deviation of the CV curves under bending even rolling states, which could strongly signify the stable and reliable performance.

For further characterize the shape effect on performance, square-shaped MSC (S-MSC) has been compared with C-MSC through CV curves (200 mV/s) and GCD curves (0.5 μA) (Fig. 6(a-b)). As the areal capacitance is the most precise characterization for evaluating the charge-storage capacity of MSC, the areal capacitance is obtained according to the following equation (1) based on the CV curves of both the S-MSC and C-MSC:

$$C_A = \frac{Q}{A \cdot \Delta V} = \frac{1}{k \cdot A \cdot \Delta V} \int_{V_1}^{V_2} I(V) dV \quad (1)$$

where,  $C_A$  is the areal capacitance,  $I(V)$  is the discharge current function,  $k$  is the scan rate,  $A$  is the effective area of the MSC.  $\Delta V$  is the potential window during the discharging process, where  $V_1$  and  $V_2$  are maximum and minimum voltage values, respectively. Fig. 6(c) compares the areal capacitances of S-MSC and C-MSC at various

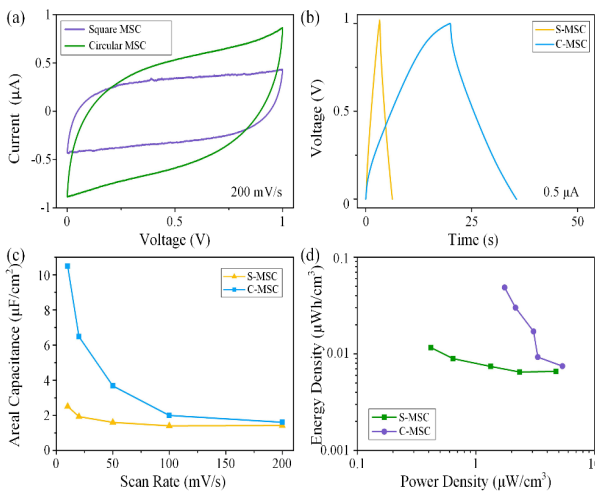


**Figure 6: Electrochemical performance comparison between square and circular MSCs on the paper substrate.**

scan rates. At the scan rate of 10 mV/s, the C-MSC and S-MSC could achieve the maximum areal capacitance of 10.491 μF/cm<sup>2</sup> and 2.508 μF/cm<sup>2</sup>, respectively, which decreases with the increase of the scan rate on account of the reduced charge responsiveness.

As for the Ragone plots (Fig. 6(d)), the volumetric energy and power density of S-MSC and C-MSC are calculated from CV curves at the voltage scan rate of 10 mV/s to 200 mV/s. Both of them could be achieved by the following equations:

$$E = \frac{1}{2 \times 3600} C_V (\Delta V)^2 \quad (2)$$

$$P = \frac{E}{\Delta t} \times 3600 \quad (3)$$

where,  $C_V$  is the volumetric capacitance obtained by dividing the  $C_A$  by the thickness of 500 μm,  $\Delta t$  is the discharging time,  $E$  is the energy density and  $P$  is the power density, respectively. The highest energy density of the C-MSC is 0.049 μWh/cm<sup>3</sup> at the scan rate of 10 mV/s, while the highest power density is 5.369 μW/cm<sup>3</sup> at the scan rate of 200 mV/s. It is worth noting that the S-MSC delivers relatively low performance due to the comparatively low areal utilization ratio of electrodes.

Additionally, in order to prove the reliability of fabrication on different substrates, we contrast the electrochemical performance of C-MSCs on paper and other general polymer substrates, respectively. It is obvious that each C-MSC under different substrates delivers decent performance. On account of the greater roughness and relatively large specific surface area of the paper-based substrate, where the ink adheres more fully, the device exhibits superior performance. The diversified choices of substrates is featured prominently in our gravure printing process, which shows great enhancement in its versatility.

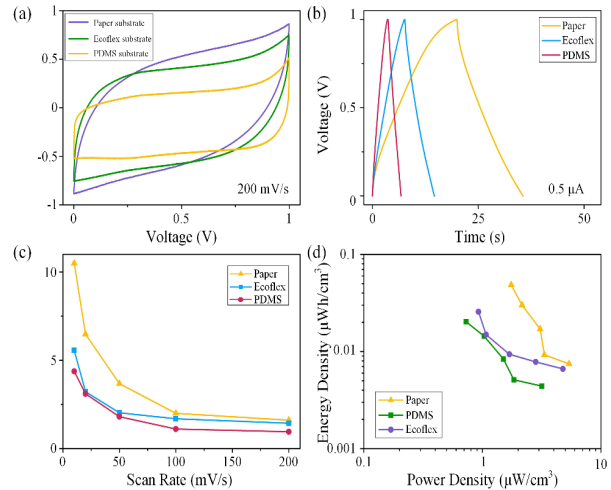


**Figure 7: Electrochemical performance comparison between square MSCs on the different substrates.**

## CONCLUSIONS

In summary, we present a scalable and general fabrication for MSCs among various flexible substrates assisted by the stamp, which combines the conductive polymer composites with gravure printing process. The excellent electrical property of CNTs and the intrinsic

flexibility of PDMS are responsible for the elegant areal capacitance ( $10.491 \mu\text{F}/\text{cm}^2$ ) of C-MSCs on the paper substrate, which maintains more than 90% after 2,000 charging-discharging cycles. Enhancing the interaction between ink and substrate plays a crucial role in improving the gravure printing resolution, which could be effectively solved by modulating the ratio of matrix and curing agent of PDMS contained in ink. Such printing technology, as a solution-based processing method, could realize high yield without the extra equipment while mitigating the mechanical damage during the preparation. Therefore, such general fabrication technology with simplified methods significantly improves the production efficiency as well as caters the requirements of modernization of MSCs.

## ACKNOWLEDGEMENTS

This work is supported by National Natural Science Foundation of China (Grant No. 61674004).

## REFERENCES

- [1] M. Stoppa and A. Chiolerio, "Wearable electronics and smart textiles: a critical review.", *sensors*, vol. 14, pp. 11957-11992, 2014.
- [2] W. Zeng, L. Shu, Q. Li, S. Chen and F. Wang, "Fiber-based wearable electronics: a review of materials, fabrication, devices, and applications.", *Adv. Mater.*, vol. 26, pp. 5310-5336, 2014.
- [3] X. Zhang, M. Han, B. Kim, J. Bao, J. Brugger, H. Zhang, "All-in-one self-powered flexible microsystems based on triboelectric nanogenerators.", *Nano Energy*, vol. 47, pp. 410-426, 2018.
- [4] Y. Song, H. Wang, X. Cheng, G. Li, X. Chen, H. Chen, L. Miao, X. Zhang and H. Zhang, "High-efficiency self-charging smart bracelet for portable electronics", *Nano Energy*, vol. 55, pp. 29-36, 2019.
- [5] Y. Song, J. Zhang, H. Guo, X. Chen, Z. Su, H. Chen, X. Cheng and H. Zhang, "All-fabric-based wearable self-charging power cloth", *Appl. Phys. Lett.*, vol. 111, 073901, 2017.
- [6] X. Pu, L. Li, H. Song, C. Du, Z. Zhao, C. Jiang and Z. Wang, "A self-charging power unit by integration of a textile triboelectric nanogenerator and a flexible lithium-ion battery for wearable electronics.", *Adv. Mater.*, vol. 27, pp. 2472-2478, 2015.
- [7] Y. Song, X. Cheng, H. Chen, M. Han, X. Chen, J. Huang, Z. Su and H. Zhang, "Highly compression - tolerant folded carbon nanotube/paper as solid-state supercapacitor electrode", *Micro Nano Lett.*, vol. 11, pp. 586-590, 2016.
- [8] Y. Song, X. Cheng, H. Chen, J. Huang, X. Chen, M. Han, Z. Su, B. Meng, Z. Song and H. Zhang, "Integrated self-charging power unit with flexible supercapacitor and triboelectric nanogenerator", *J. Mater. Chem. A*, vol. 4, pp. 14298-14306, 2016.
- [9] L. Kou, T. Huang, B. Zheng, Y. Han, X. Zhao and C. Gao, "Coaxial wet-spun yarn supercapacitors for high-energy density and safe wearable electronics.", *Nat. Commun.*, vol. 5, 3754, 2014.
- [10] X. Yu, B. Lu and Z. Xu, "Super long-life supercapacitors based on the construction of nanohoneycomb-like strongly coupled CoMoO<sub>4</sub>-3D graphene hybrid electrodes.", *Adv. Mater.*, vol. 26, pp.1044-1051, 2014
- [11] F. Simjee and P. Chou, "Efficient charging of supercapacitors for extended lifetime of wireless sensor nodes.", *IEEE T. Power Electr.*, vol. 23, pp.1526-1536, 2008.
- [12] Y. Song, X. Chen, J. Zhang, X. Cheng and H. Zhang, "Freestanding micro-supercapacitor with interdigital electrodes for low-power electronic systems", *J. Microelectromech. Syst.*, vol. 26, pp. 1055-1062, 2017.
- [13] J. Sun, B. Cui, F. Chu, C. Yun, M. He, L. Li and Y. Song, "Printable nanomaterials for the fabrication of high-performance supercapacitors.", *Nanomaterials*, vol. 8, 528, 2018.
- [14] J. Hwang, S. Cho, J. Dang, E. Kwak and K. Song, "Direct nanoprinting by liquid-bridge-mediated nanotransfer moulding.", *Nat. Nanotechnol.*, vol. 5, pp. 742-748, 2010.
- [15] H. Zhang, A. Ramm, S. Lim, W. Xie and B. Ahn, "Wettability contrast gravure printing.", *Adv. Mater.*, vol. 27, pp. 7420-7425, 2015.
- [16] J. Cen, R. Kitsomboonloha and V. Subramanian, "Cell filling in gravure printing for printed electronics.", *Langmuir*, vol. 30, pp. 13716-13726, 2014.
- [17] Y. Song, H. Chen, Z. Su, X. Chen, L. Miao, J. Zhang, X. Cheng and H. Zhang, "Highly compressible integrated supercapacitor-piezoresistance-sensor system with CNT-PDMS sponge for health monitoring", *Small*, vol. 13, 1702091, 2017.
- [18] Y. Song, H. Chen, X. Chen, H. Wu, H. Guo and X. Cheng, "All-in-one piezoresistive-sensing patch integrated with micro-supercapacitor.", *Nano Energy*, vol. 53, pp. 189-197, 2018.
- [19] R. Kitsomboonloha and V. Subramanian, "Lubrication-related residue as a fundamental process scaling limit to gravure printed electronics.", *Langmuir*, vol. pp. 3612-3624, 2014.

## CONTACT

\*H.X. Zhang, hxzhang@pku.edu.cn

†These authors contribute equally.